

NJC

Accepted Manuscript



This is an *Accepted Manuscript*, which has been through the Royal Society of Chemistry peer review process and has been accepted for publication.

Accepted Manuscripts are published online shortly after acceptance, before technical editing, formatting and proof reading. Using this free service, authors can make their results available to the community, in citable form, before we publish the edited article. We will replace this *Accepted Manuscript* with the edited and formatted *Advance Article* as soon as it is available.

You can find more information about *Accepted Manuscripts* in the [Information for Authors](#).

Please note that technical editing may introduce minor changes to the text and/or graphics, which may alter content. The journal's standard [Terms & Conditions](#) and the [Ethical guidelines](#) still apply. In no event shall the Royal Society of Chemistry be held responsible for any errors or omissions in this *Accepted Manuscript* or any consequences arising from the use of any information it contains.

Nano-MoO₃ mediated synthesis of bioactive thiazolidin-4-ones acting as anti-bacterial agents and their mode-of-action analysis using *in silico* target prediction, docking and similarity searching

Keerthy Hosadurga Kumar,^a Shardul Paricharak,^{b,c} Chakrabhavi Dhananjaya Mohan,^d Hanumantharayappa Bharathkumar,^a Nagabhushana GP,^e Dinesh Koragere Rajashekar,^a Gujjarahalli Thimmanna Chandrappa,^e Andreas Bender,^{b,*} Basappa,^{a,*} Kanchugarakoppal Subbegowda Rangappa^{d,*}

^a*Laboratory of Chemical Biology, Department of Chemistry, Bangalore University, Bangalore-560001, India*

^b*Centre for Molecular Informatics, Department of Chemistry, Cambridge, CB2 1EW, United Kingdom*

^c*Division of Medicinal Chemistry, Leiden Academic Centre for Drug Research, Leiden University, P.O. Box 9502, 2300 RA Leiden, The Netherlands*

^d*Department of Studies in Chemistry, University of Mysore, Manasagangotri, Mysore-570 006, India*

^e*Department of Chemistry, Bangalore University, Bangalore-560001, India*

***Corresponding Authors**

Abstract

The efficacy of thiazolidin-4-ones as synthons for diverse biological small molecules has given impetus to antibacterial studies. Our work aims to synthesize novel bioactive thiazolidin-4-ones using nano-MoO₃ for the first time. The compelling advantage of using nano-MoO₃ is that the recovered nano-MoO₃ can be re-used thrice without considerable loss of its catalytic activity. The synthesized thiazolidin-4-ones were tested for antibacterial activity against two strains of pathogenic bacteria namely, *Salmonella typhi* and *Klebsiella pneumoniae*. Our results indicated that compound **3b** showed significant inhibitory activity towards *Salmonella typhi*, in comparison with gentamicin. Furthermore, *in silico* target prediction presented the target of compound **3b** as FtsK motor domain of DNA translocase of *Salmonella typhi*. Hence, our hypothesis is that compound **3b** may disrupt the chromosomal segregation and thereby inhibit the division of *Salmonella typhi*. In addition, similarity searching showed that 34 compounds with a chemical similarity of 70% or higher to compound **3b**, which were retrieved from ChEMBL, bound to targets associated with biological processes related to cell development in 36% of the cases. In summary, our work details novel usage of nano-MoO₃ for the synthesis of novel thiazolidin-4-ones possessing anti-bacterial activity, and present a mode-of-action hypothesis.

Introduction

Transition metal oxides are extensively used in many organic reactions owing to their advantage over their counterparts.¹ The use of co-ordination compounds with variety of metals have replaced acids or bases with satisfactory yields. Often, use of acid or bases results in low product yield due to reverse/side reactions and the use of organic solvents increases the difficulty

in catalyst recovery.² Molybdenum oxide (MoO_3) is projected as potential nanostructure because of its wide range of stoichiometric, structural, thermal, chemical and optical properties.³⁻⁵ MoO_2 or MoO_3 supported catalysts are reported to efficiently catalyze various organic reactions including Beckmann rearrangement,⁶ nitration of aromatics,⁷ oxidation of ammonia to elemental N_2 and synthesis of diphenyl carbonate from dimethyl carbonate and phenol.⁸ In the present work, we report the use MoO_3 for the synthesis of novel thiazolidin-4-ones and analyzed the anti-bacterial activity of new structures.

Antibiotic resistance is a major concern in contemporary medicine and has emerged as one of the prominent public health issues of the 21st century,⁹ particularly as it pertains to pathogenic organisms such as *Salmonella typhi* and *Klebsiella pneumoniae*.¹⁰ *S. typhi* and *K. pneumoniae* are the pathogenic gram-negative bacterial strains, where former is predominately found in the intestinal lumen and latter in the gastrointestinal tract and in naso-pharynx.

Diverse species of pathogenic gram-negative bacteria use secretion systems to export a variety of protein toxins and virulence factors that help to establish and maintain infection. Disruption of such secretion systems is a potentially effective therapeutic strategy against these bacterial infections. In order to develop small molecule antibacterials, we subjected the title compounds to a high-throughput screen and identified a tris-aryl substituted 2-imino-5-arylidene-thiazolidin-4-one, compound **3b**, as an inhibitor of the Type III secretion system. Expansion of this chemotype enabled us to define the essential pharmacophore for Type III secretion inhibition by this structural class.^{11, 12}

In continuation of our work to synthesize and explore pharmacological properties of various class of heterocycles,¹³⁻²⁰ herein we report the application of MoO_3 nanoparticles in the synthesis of novel thiazolidin-4-ones, followed by their use as antibacterial agents against *S. typhi*

and *K. pneumoniae*. Furthermore, we used chemogenomics approaches to predict protein targets *in silico* and rationalized the mode-of-action of the bioactive thiazolidin-4-one.

Result and Discussion

Characterization of nano-MoO₃:

The powder XRD pattern was recorded on a PANalytical X'pert PRO X-ray diffractometer with a graphite monochromatized Cu K α radiation source ($\lambda=1.541$ °Å). Morphologies and particle sizes of combustion-derived powders were examined using a JEOL-JSM-6490 LV scanning electron microscope (SEM) and a transmission electron microscope (TEM) by JEOL JEM 2100 operating at 200 kV.

The powder X-ray diffraction patterns, SEM image and TEM image of nano MoO₃ are shown in figure 1a-c and are reported.²¹

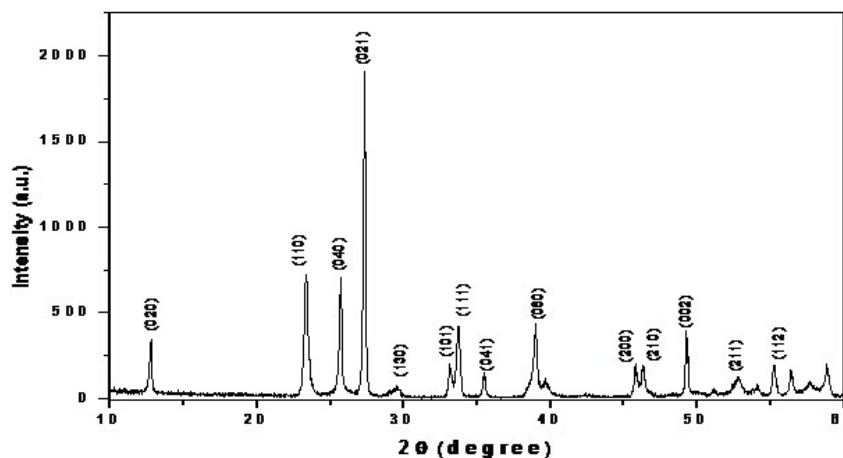


Figure 1: (a) PXRD patterns of MoO₃ powders

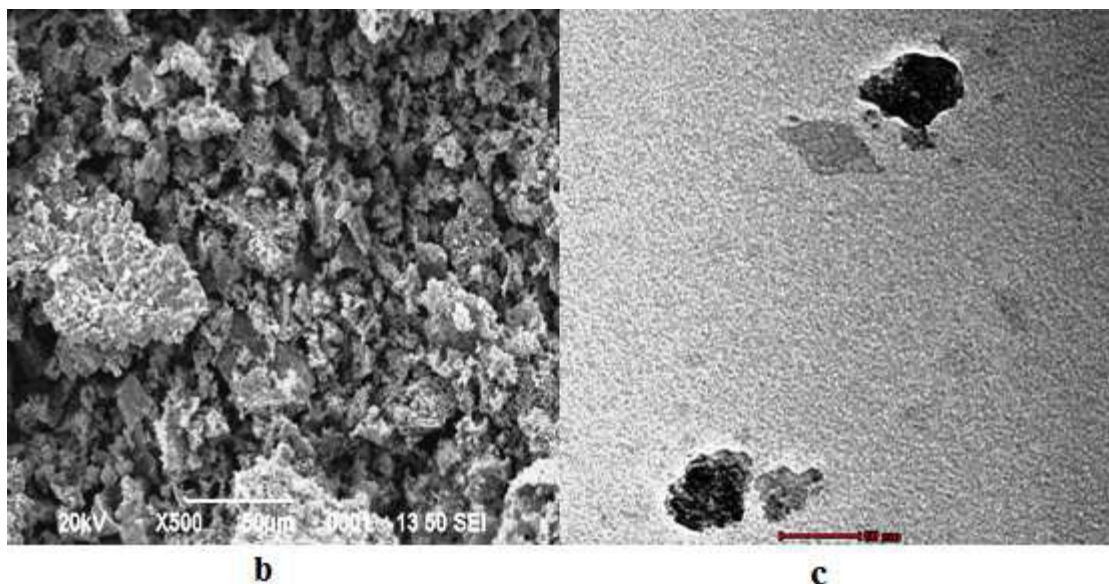
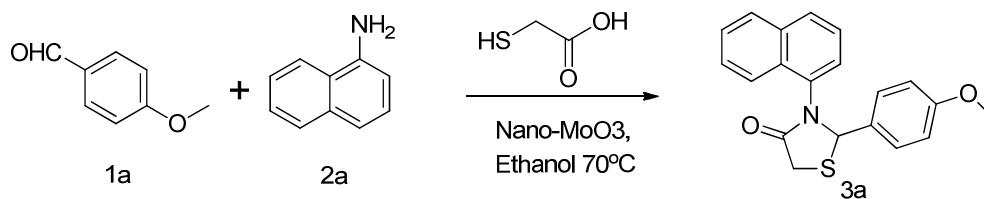


Figure 1: (b) SEM image of MoO₃ (c) TEM image of MoO₃

Selection of the reaction system and optimization of reaction conditions:

Initially, we synthesized thiazolidin-4-ones by the reaction of p-anisaldehyde (1a) with β -naphthyl amine (2a) using various methodologies as reported in table 1 and came up with a stabilized protocol using MoO₃



Scheme 1a: Synthesis of 2-(4-methoxyphenyl)-3-(naphthalen-1-yl)thiazolidin-4-one²²

We found that the use of nano MoO₃ in ethanol is the system ideal for the ring forming condensation reaction. The reactions with other methodologies resulted in low yields, while nano-MoO₃ in refluxing ethanol led to comparatively high yield of the product.

Table 1: Comparative study on different methods and solvent for thiazolidin-4-one formation.

Sl. No.	Method	Solvent	Temperature (°C)	Amount of reagent (eq)	Yield ^a (%)	Time (Hrs)
1	ZnCl ₂	Ethanol	80	2	71	32
2	Dean-Stark's	Toluene	110	-	78	48
3	DCC	THF	0-25	2.5	67	2.5
4	T3P	Ethyl Acetate: DMSO	0-25	2.5	82	6
5	Nano MoO₃	Ethanol	70	1.8	94	4

DCC-N, N'-Dicyclohexylcarbodiimide, THF- Tetrahydrofuran, T3P- Propylphosphonic anhydride

Ethanol as the ideal reaction media and re-usability of the acidic nano MoO₃

To achieve a stabilized reaction system for thiazolidin-4-ones synthesis, we considered the reaction between p-anisaldehyde (1 eq) (1a) and β-naphthyl amine (1 eq) (2a) (Scheme 1a). The reaction between 1a and 2a in the presence of nano MoO₃ (1 eq) in ethanol at 70 °C resulted in the product (3a) yield of 52% after 6.2 h (Table 2, entry 1). The increase in the amount of nano MoO₃ (1.8 eq) resulted in the increase of product yield to 94% within 4 h (Table 2, entry 2 & 3). Further increase in the amount of nano MoO₃ in the reaction does not affect the reaction time and yield (Table 2, entry 4). The presence of vacant d-orbital molybdenum oxide facilitates the formation of arylimine intermediate between 1a and 2a, and its acidic nature facilitates the process of cyclization of arylimine and thioglycolic acid forming the product 3a.

Subsequently, we attempted to explore a better solvent system for the reaction with various polar and non-polar solvents. The reaction was monitored in solvents such as acetonitrile: water,

ethanol : water, n-butanol, THF, benzene and toluene. All the tested solvent systems displayed an inferior product yield (3a) than that of ethanol (Table 2 entries 5-11).

Table 2: Nano-MoO₃ catalyzed synthesis of compound **3a** under different reaction conditions.

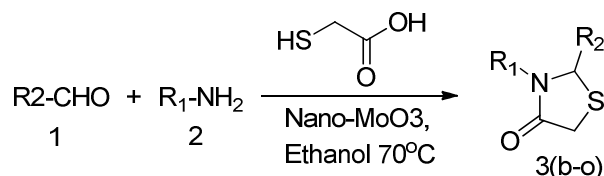
Entry	Solvent	Nano MoO ₃ (equiv)	Time (h)	Temperature (°C)	Yield ^a (%)
1	Ethanol	1.0	6.2	70	52
2	Ethanol	1.5	6	70	70
3	Ethanol	1.8	4	70	94
4	Acetonitrile:Water (8:2)	1.8	10	75	Traces
5	Ethanol:Water (8:2)	1.8	12	80	Traces
6	n-Butanol	1.8	9	110	78
7	THF	1.8	8.5	65	72
8	Benzene	1.8	42	80	63
9	Toulene	1.8	36.	110	58
10	Acetonitrile	1.8	7.5	70	82

^aYield of the product after column chromatography.

We next analyzed the reusability of nano MoO₃, which was used in the synthesis of thiazolidin-4-one as represented in scheme 1a. After the completion of reaction every time, filtered residue containing nano MoO₃ was washed with ethanol and reused for next run with fresh p-anisaldehyde, 2-naphthyl amine and thiaglycolic acid. We observed the considerable decrease in the yield of the product on reuse of nano MoO₃ after third run. The second and third run resulted in the yield of 74 % and 65 % respectively.

We finally used the optimized reaction conditions to prepare the novel series of thiazolidin-4-ones in which we used aryl/heteroaryl aldehydes with heteroaryl amines and

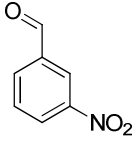
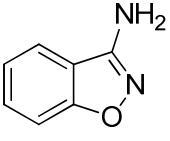
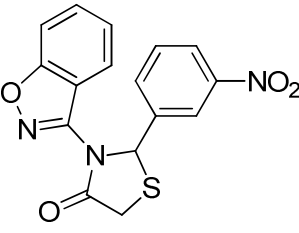
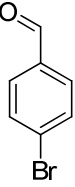
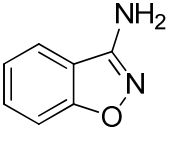
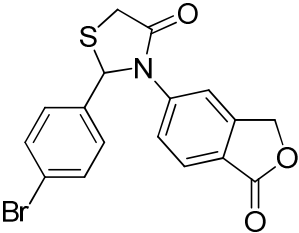
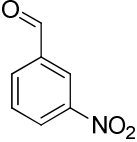
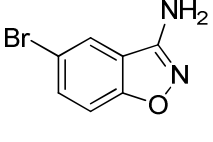
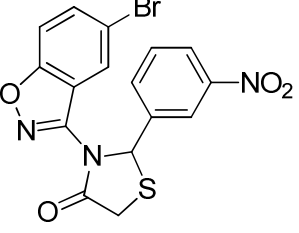
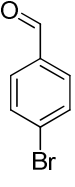
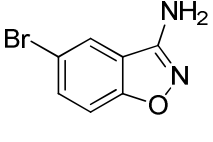
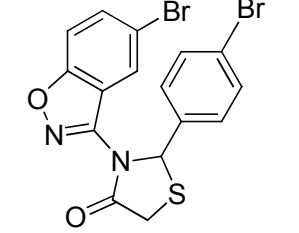
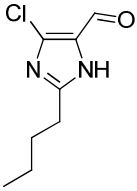
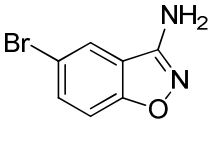
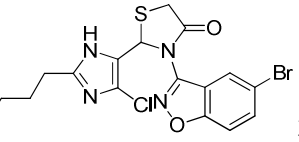
thioglycolic acid (Scheme 1b). Most of the aldehydes and amines bearing various electron donating and electron withdrawing substituents resulted in products with high yields (Table 2 entries 2-15).

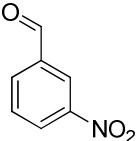
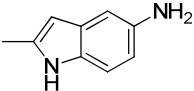
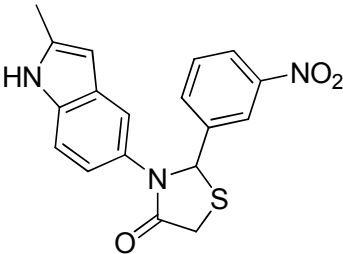
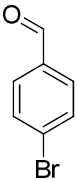
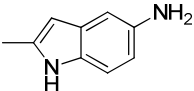
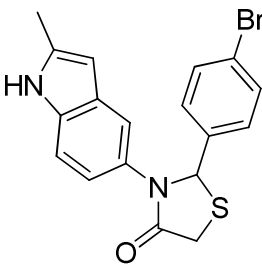
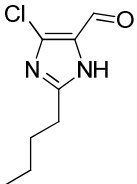
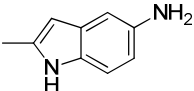
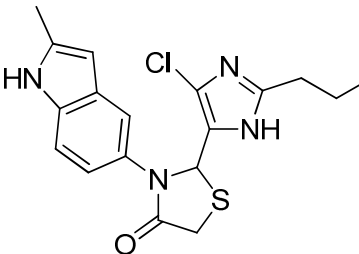
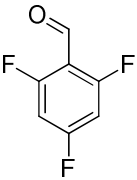
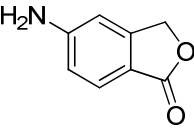
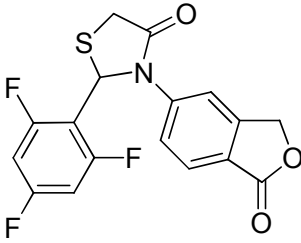


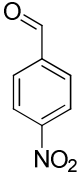
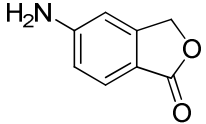
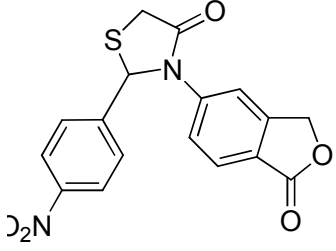
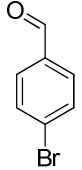
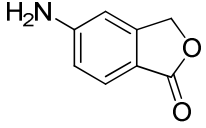
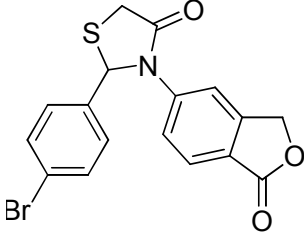
Scheme 1b: Synthesis of novel series of thiazolidin-4-ones 3(b-o).

Table 3: Novel thiazolidin-4-ones synthesized using nano MoO₃.

Entry ^a	Aldehyde(1)	Amine(2)	3(b-o)	Time(h)	Yield ^b (%)
1				3	96
2				2.5	90
3				2.5	93

4				3	91
5				3.5	89
6				4	90
7				3	92
8				5	86

9				3.5	92
			3j		
10				3	93
			3k		
11				4.5	88
			3l		
12				4	90
			3m		

13				3	92
14				3.5	91

^aConditions: aldehyde : amine : thioglycic acid; Nano MoO₃=1:1:1.5:1.8 (eq)

^bIsolated yield after column chromatography.

Anti-bacterial activity

The minimum inhibitory concentration (MIC) of the compound, which is required for inhibition of bacterial growth by the compounds 3(a-o), along with the MIC of a reference drug (Gentamicin) are shown in Table 4. Our results show that, of the benzisoxazole and indole series, compound **3b**, **3c** (benzisoxazole series) and compound **3l** (indole series) showed significant anti-bacterial activity towards *S. typhi* with zone of inhibition values of 23 mm, 17 mm and 16 mm, respectively and MIC values of 300 µg/mL, 400 µg/ml and 800 µg/ml respectively. Compounds 3e and 3l were found to be effective against *K. pneumoniae* with zone of inhibition values of 14 mm and 14 mm, respectively, and MIC values of 700 µg/ml and 400 µg/ml respectively.

Table 4: Antibacterial activities-Zone of Inhibition of thiazolidin-4-ones 3(b-o) towards *S. typhi*, and *K. pneumoniae*

Compounds	<i>Klebsiella pneumoniae</i> Zone of inhibition in mm	<i>Salmonella typhi</i> Zone of inhibition in mm
3b	14	23
3c	14	17
3d	NA ^a	NA ^a
3e	12	NA ^a
3f	14	11
3g	NA	NA
3h	16	12
3i	12	16
3j	14	24
3k	NA ^a	NA ^a
3l	14	16
3m	12	11
3n	14	15
3o	18	13
Gentamicin	32	35
^a NA: not active		

Cheminformatics

Human protein targets were predicted for the most bioactive compound **3b**, which was shown to have an inhibitory effect on the growth of *S. Typhi*.²³ The predicted target, Potassium voltage-gated channel subfamily A member 5, with a corresponding probability value of 0.069 is shown in Table 5. In addition, the occurrence of Potassium voltage-gated channel subfamily A member 5 in the background dataset was measured. It was found that the Potassium voltage-gated

channel subfamily A member 5 had a normalised likelihood of 5,882 for compound **3b**, meaning that this prediction is very unlikely to have occurred by chance alone. Given that the predicted protein Potassium voltage-gated channel subfamily A member 5 is a human protein, a DELTA-BLAST search was performed on the predicted target protein in order to find orthologous proteins in *S.typhi* (results shown in Table 6). We found that the predicted target ‘Potassium voltage-gated channel subfamily A member 5 had sequence homology to the *S.typhi* proteins Putative surface-exposed virulence protein BigA (Uniprot ID: P25927.2), Proline-specific permease ProY (Uniprot ID: P37460.3) and DNA translocase FtsK (Uniprot ID: Q8ZQD5.1) with e-values of $3 \cdot 10^{-6}$, $3 \cdot 10^{-4}$ and 0.002 respectively. Given that the Putative surface-exposed virulence protein BigA (Uniprot ID: P25927.2) is involved in virulence of bacteria and that the Proline-specific permease ProY (Uniprot ID: P37460.3) is the structural gene for a cryptic proline transporter,^{24, 25} we hypothesise the latter target, the DNA translocase FtsK (Uniprot ID: Q8ZQD5.1) as potentially being the target that is responsible for growth inhibition of *S.typhi*.

In addition, in order to investigate the bioactivity profile of compounds similar to compound **3b** and thus to understand the target prediction of compound **3b** from the chemical side, bioactivity data was retrieved for 34 compounds from ChEMBL with a similarity of 70% or higher to compound **3b**, covering 39 unique protein targets. Of these, 32 targets had a PANTHER²⁶ ‘biological process’ annotation. It can be seen that in 36% of the cases, the proteins are associated with the terms ‘Cellular process’, ‘Cell communication’, ‘Cell cycle’, ‘Cellular component organization’ or ‘Apoptosis’. These results indicate that compounds similar to compound **3b** could very well be involved in the disruption of cellular development, and hence, are in agreement with our prediction that DNA translocase FtsK is the mode-of-action of compound **3b**, as DNA translocase FtsK is also of importance in cellular development.^{27, 28}

Table 5: *In Silico* human target predictions are listed for thiazolidin-4-ones on the Parzen-Rosenblatt Window classifier.

Compound	Predicted Target 1 (PRW)	Uniprot ID	Probability	Predicted Target 1 (NB)	Uniprot ID	Probability
3b	Potassium voltage-gated channel subfamily A member 5	P22460	0.069	Endothelin B receptor	<u>P24530</u>	6.60
3c	Sigma non-opioid intracellular receptor 1	Q99720	0.052	Receptor-type tyrosine-protein kinase FLT3	<u>P36888</u>	5.82
3d	Sigma non-opioid intracellular receptor 1	Q99720	0.053	Receptor-type tyrosine-protein kinase FLT3	<u>P36888</u>	5.92
3e	Sigma non-opioid intracellular receptor 1	Q99720	0.06	Receptor-type tyrosine-protein kinase FLT3	<u>P36888</u>	7.42
3f	Prostaglandin G/H synthase 2	P23219	0.05	Potassium voltage-gated channel subfamily A member 5	P22460	5.55
3g	Sigma non-opioid intracellular receptor 1	Q99720	0.079	1-acyl-sn-glycerol-3-phosphate acyltransferase beta	O15120	10.33
3i	Carbonic anhydrase 2	P00918	0.083	Type-2 angiotensin II receptor	P50052	9.59
3j	Prostaglandin G/H synthase	P23219	0.112	TGF-beta receptor type-1	P36897	7.61
3k	Prostaglandin G/H synthase	P23219	0.1	Tyrosine-protein kinase ITK/TSK	Q08881	7.38
3l	Carbonic anhydrase 2	P00918	0.061	Type-1 angiotensin II receptor"		21.59

Table 6: DELTA-BLAST results for the Potassium voltage-gated channel subfamily A member 5.

# blastp											
# Iteration: 1											
# Query: gi 146345443 sp P22460.4 KCNA5_HUMAN Potassium voltage-gated channel subfamily A member 5											
# Database: swissprot											
Hit ID	% identity	% positives	alignment length	Mismatches	gaps	q.start	q.end	s.start	s.end	e-value	bit score
Putative surface-exposed virulence protein BigA	14.29	24.76	105	89	1	5	109	107	210	3.00E-06	46.2
Putative surface-exposed virulence protein BigA	12.96	24.07	108	88	2	5	106	116	223	5.00E-05	42.4
Putative surface-exposed virulence protein BigA	15.45	27.27	110	85	2	5	106	125	234	8.00E-05	41.6
Putative surface-exposed virulence protein BigA	15.53	24.27	103	80	2	6	106	82	179	0.002	37
Putative surface-exposed virulence protein BigA	12.5	21.59	88	74	1	32	116	94	181	0.003	36.6
Putative surface-exposed virulence protein BigA	11.24	17.98	89	72	2	28	109	78	166	0.033	33.1
Proline-specific permease ProY	10.71	37.5	112	89	2	421	527	320	425	3.00E-04	39.3
DNA translocase FtsK	11.49	18.39	87	72	2	18	99	393	479	0.002	37.4
DNA translocase FtsK	17.89	26.32	95	73	2	16	105	401	495	0.01	34.7

Rationalization of the putative target of the bioactive thiazolidin-4-ones via *in silico* molecular docking

Given that our cheminformatics approaches present the predicted putative target, namely the DNA translocase FtsK, as a mode-of-action hypothesis, we subsequently performed molecular docking studies to understand the ligand-protein interactions in detail. FtsK is a conserved DNA translocase, whose action is crucial in bacterial cell division during the late stages of chromosome segregation.^{29, 30 18, 19}. In addition, deletion or over expression of FtsK can result in the inhibition of cell division.²⁰ The docking scores (DS) of the docked compounds with the FtsK motor domain are summarised Table 7. The thiazolidin-4-one derivatives show DS scores higher than 50 and are therefore likely to interact with the FtsK motor domain based on this model

(Table 4). Furthermore, compounds **3b** and **3l** (Both in S-form) from the benzisoxazole and the indole series were shown to likely interact with the hydrophilic pocket of the FtsK motor domain with a high DS of 64.6 and 50.4, respectively. Figures 2 and 3 represent the comparative interaction map of the compounds **3b** and **3l** with the hydrophobic site of FtsK motor domain, respectively. The interaction between both compounds and FtsK can be viewed in terms of their binding to three clusters of the FtsK motor domain. The amino acids Lys1183, Arg1187, Asn908, Ala904 and Ser907 of the FtsK motor domain are predicted to interact with the benzisoxazole or indole rings, whereas the amino acids Glu1196, Gly1194, Gln1192, Ala1193, and Val924 appear to interact with the thiazolidin-4-one nucleus. The third cluster consisted of the amino acids Pro1214, Arg1216, Leu1213, Val1215, Glu926, Val925, Val927 and Pro929 that were buried by the substituted phenyl or substituted-imidazole moiety. In addition to the fact that both compounds **3b** and **3l** are predicted to interact with the FtsK motor domain, they both inhibit bacterial growth efficiently. The potent inhibition of compound **3b** towards the growth of *S.typhi* might hence be due to the strong and unique hydrogen bonding between the amino acids Lys1183, Arg1187 and benzisoxazole heteroatoms and also between the amino acid Arg 923 and the methoxy-phenyl group of compound **3b**. In short, the interactions predicted between compound **3b** and the FtsK motor domain are representative for other putative inhibitors of the same domain.

Table 7: Predicted binding energies of thiazolidin-4-ones with FtsK DNA translocase.

Compounds	MW	-PLP1	-PLP2	DS	LIE
3b	326.37	80.82	78.77	64.622	-1.458
3j	353.39	76.9	65.06	47.504	-2.452
3k	387.29	75.39	65.47	47.539	-2.246
3l	388.91	70.78	60.03	50.354	-6.210
3i	455.67	53.45	46.78	52.749	-7.170

MW: Molecular Weight, PLP1: Piecewise Linear Potential1, PLP2: Piecewise Linear Potential2, LIE: ligand internal energy, DS: Docking Score

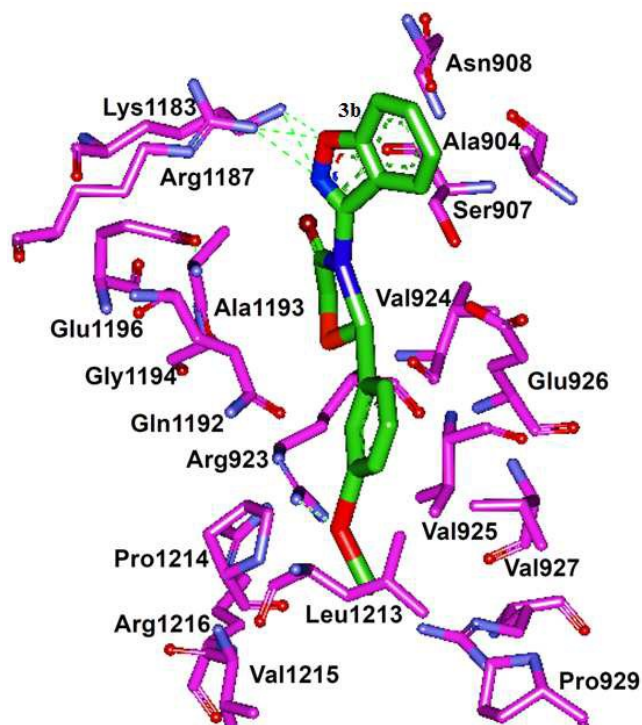


Figure 2: Interaction map showing the key amino acids of the FtsK motor domain of *S. typhi* bound to compound **3b**

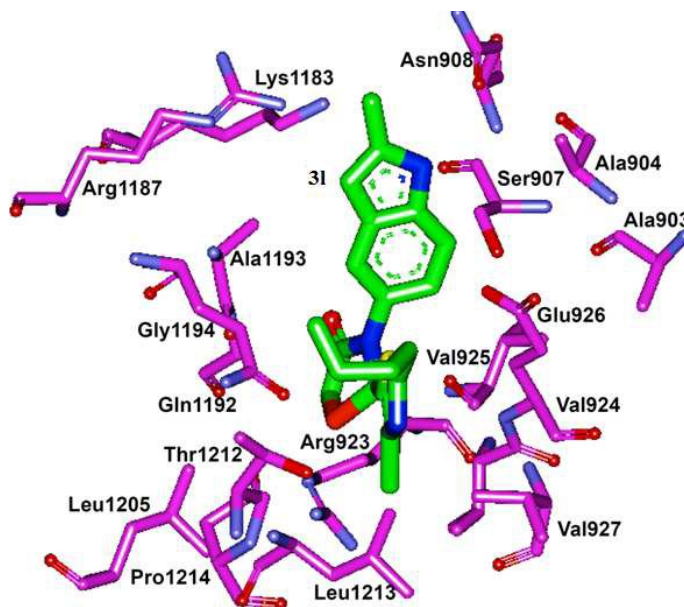


Figure 3: Interaction map showing the key amino acids of the FtsK motor domain of *S. typhi* bound to compound **3l**

Conclusions

In this study, we developed synthetic method for novel bioactive thiazolidine-4-ones by condensation of aryl/heteroaryl aldehydes, heteroaryl amines using nano MoO₃ for the first time. The antibacterial activity of the synthesised thiazolidin-4-ones against two pathogenic strains, namely *S.typhi* and *K.pneumoniae* revealed that compound 3b showed significant inhibitory activity towards *S.typhi*, with an activity comparable to gentamicin. Furthermore, *in silico* human target prediction for compound 3b predicted the FtsK domain of DNA translocase as a putative target. In addition, our molecular docking analysis suggests that the highly active compound 3b strongly interacts with the FtsK motor domain, when compared to other structurally related compounds, hereby indicating that it may disrupt chromosome segregation and thereby inhibit the cell division of *S.typhi* in culture.

Experimental Section

Synthesis of nano-MoO₃

Nano MoO₃ has been synthesized according to reported procedure.²¹

Synthesis of novel thiazolidin-4-ones

All reagents were commercially available reagent grade and were used without further purification. Thin layer chromatography (TLC) was conducted on 0.25 mm silica gel plates (60F254, Merck). Column chromatography separations were obtained on silica gel (200-400 mesh). IR spectra were recorded on Bruker FTIR spectrophotometer. ¹H NMR spectra were recorded on a BrukerAvance-400 instrument (few on Agilent NMR instrument) in DMSO-d₆ (few in CDCl₃) solvent. ¹³C NMR spectra were obtained on an Agilent NMR instrument at 100 MHz in DMSO-d₆ solvent (few in CDCl₃). Chemical shifts were expressed in ppm downfield

relative to TMS. Mass spectra were recorded on an Agilent LC-MS. The elemental analysis was carried out using an Elemental Vario Micro Cube CHN analyzer.

General procedure

Aryl/heteroaryl aldehyde (1 eq), heteroaryl amine (1 eq) and thioglycolic acid (1.5 eq) were refluxed in ethanol in presence of nano MoO₃ (1.8 eq) for stipulated time (Table 3). Reaction was monitored for its completion by thin layer chromatography using hexane:ethylacetate (7:3) mobile phase. After the completion of the reaction, it is brought to room temperature, filtered through Whatman filter paper 42 and solvent was removed under vacuum to get the novel thiazolidin-4-ones (3a-o). The pure product was obtained by column chromatography using ethyl acetate and n-hexane and ethyl acetate (about 15%) as eluent.

Spectral Characterization of novel thiazolidin-4-ones 3(b-o)

3-(benzo[d]isoxazol-3-yl)-2-(3-methoxyphenyl) thiazolidine-4-one (3b):

IR (KBr): 1728 cm⁻¹ $\nu_{(C=O)}$; ¹H NMR (400 MHz, DMSO d₆ δ in ppm) δ 8.002 (s, 1H, Ar-H), 7.664-7.639 (m, 2H, Ar-H), 7.419-7.396 (m, 1H, Ar-H), 7.177-7.157 (m, 1H, Ar-H), 7.005-6.984 (m, 2H, Ar-H), 6.797-6.774 (m, 1H, Ar-H), 6.561 (s, 1H, S-CH-), 4.199-4.196 (d, J = 1.2 Hz, 1H, -CH₂-), 4.159-4.156 (d, J = 1.2 Hz, 1H, -CH₂-), 3.644 (s, 3H, -OCH₃); ¹³C NMR (100 MHz, CDCl₃ δ in ppm) δ 173.21, 163.19, 159.21, 148.11, 139.28, 130.54, 128.52, 123.91, 122.52, 120.55, 111.21, 108.57, 67.33, 55.11, 32.12; ESI-MS m/z 327 [M+H]⁺; Anal. Calcd for C₁₇H₁₄N₂O₃S: C, 62.56; H, 4.32; N, 8.58; Found C, 62.49; H, 4.26; N, 8.45%.

3-(benzo[d]isoxazol-3-yl)-2-(4-nitrophenyl) thiazolidine-4-one (3c):

IR (KBr): 1716 cm⁻¹ $\nu_{(C=O)}$; ¹H NMR (400 MHz, DMSO d₆ δ in ppm) δ ¹H NMR (400 MHz, DMSO d₆ δ in ppm) δ 8.156-8.073 (m, 2H, Ar-H), 7.769-7.747 (m, 2H, Ar-H), 7.667-7.650 (m,

2H, Ar-H), 7.432-7.407 (m, 2H, Ar-H), 6.743 (s, 1H, S-CH-), 4.244-4.242 (d, $J=0.8$ Hz, 1H, -CH₂-), 4.204-4.202 (d, $J=0.8$ Hz, 1H, -CH₂-); ¹³C NMR (100 MHz, DMSO-d₆ δ in ppm) δ 171.52, 162.51, 147.11, 146.28, 144.21, 130.74, 129.42, 123.01, 122.45, 119.42, 108.56, 74.27, 32.61; ESI-MS m/z 342 [M+H]⁺; Anal. Calcd for C₁₆H₁₁N₃O₄S: C, 56.30; H, 3.25; N, 12.31; found: C, 56.19; H, 3.18; N, 12.09%.

3-(benzo[d]isoxazol-3-yl)-2-(2-nitrophenyl) thiazolidine-4-one (3d):

IR (KBr): 1717 cm⁻¹ $\nu_{(C=O)}$; ¹H NMR (400 MHz, DMSO d₆ δ in ppm) δ 8.168-8.086 (m, 2H, Ar-H), 7.716-7.694 (m, 2H, Ar-H), 7.674-7.672 (m, 2H, Ar-H), 7.666-7.421 (m, 2H, Ar-H), 6.862 (s, 1H, S-CH-), 4.207-4.204 (d, $J=1.2$ Hz, 1H, -CH₂-), 4.166-4.163 (d, $J=1.2$ Hz, 1H, -CH₂-); ¹³C NMR (100 MHz, DMSO-d₆ δ in ppm) δ 170.34, 164.21, 149.05, 147.68, 135.01, 134.12, 130.98, 128.86, 127.20, 125.06, 123.67, 122.76, 108.51, 67.98, 33.81; ESI-MS m/z 342 [M+H]⁺; Anal. Calcd for C₁₆H₁₁N₃O₄S: C, 56.30; H, 3.25; N, 12.31; found C, 56.22; H, 3.19; N, 12.24%.

3-(benzo[d]isoxazol-3-yl)-2-(3-nitrophenyl) thiazolidine-4-one (3e):

IR (KBr): 1713 cm⁻¹ $\nu_{(C=O)}$; ¹H NMR (400 MHz, DMSO d₆ δ in ppm) δ 8.0 (s, 1H, Ar-H), 7.7-7.6 (m, 2H, Ar-H), 7.4 (m, 1H, Ar-H), 7.2-7.1 (m, 1H, Ar-H), 7.0-6.9 (m, 2H, Ar-H), 6.8 (m, 1H, Ar-H), 6.5 (s, 1H, S-CH-), 4.2 (d, 1H, -CH₂-), 4.1 (d, 1H, -CH₂-); ¹³C NMR (100 MHz, DMSO-d₆ δ in ppm) δ 170.23, 164.12, 147.21, 146.91, 140.86, 133.64, 130.12, 129.04, 124.85, 123.28, 122.6, 121.52, 108.62, 72.53, 34.01; ESI-MS m/z 342 [M+H]⁺; Anal. Calcd for C₁₆H₁₁N₃O₄S requires C, 56.30; H, 3.25; N, 12.31; found C, 56.26; H, 3.13; N, 12.25%.

3-(benzo[d]isoxazol-3-yl)-2-(4-fluorophenyl) thiazolidine-4-one (3f):

IR (KBr): 1720 cm⁻¹ $\nu_{(C=O)}$; ¹H NMR (400 MHz, DMSO d₆ δ in ppm) δ 7.977 (s, 1H, Ar-H), 7.655-7.636 (m, 2H, Ar-H), 7.544-7.509 (m, 2H, Ar-H), 7.410-7.075 (m, 2H, Ar-H), 6.597 (s,

¹H, S-CH-), 4.206-4.204 (d, $J=0.8$ Hz, 1H,-CH₂-), 4.166-4.164 (d, $J=0.8$ Hz, 1H,-CH₂-); ¹³C NMR (100 MHz, DMSO-d₆ δ in ppm) δ 170.15, 165.11, 159.25, 145.12, 134.24, 130.28, 123.55, 122.91, 121.46, 116.38, 115.12, 108.21, 72.21, 34.15; ESI-MS m/z 315 [M+H]⁺; Anal. Calcd for C₁₆H₁₁FN₂O₂S: C, 61.14; H, 3.53; N, 8.91; found: C, 61.05; H, 3.42; N, 8.87%.

3-(5-bromobenzo[d]isoxazol-3-yl)-2-(3-nitrophenyl) thiazolidine-4-one (3g):

IR (KBr): 1719 cm⁻¹ $\nu_{(C=O)}$; ¹H NMR (400 MHz, DMSO d₆ δ in ppm) δ 8.0-6.7 (m, 7H, Ar-H), 6.5 (s, 1H, S-CH-), 4.2 (d, 1H,-CH₂-), 4.1 (d, 1H,-CH₂-); ¹³C NMR (100 MHz, DMSO-d₆ δ in ppm) δ 170.21, 163.71, 148.12, 145.28, 139.71, 134.18, 132.12, 128.12, 125.31, 124.11, 119.37, 115.11, 112.55, 65.17, 35.28; ESI-MS m/z 419 [M+H]⁺; Anal. Calcd for C₁₆H₁₀BrN₃O₄S: C, 45.73; H, 2.40; N, 10.00; found C, 45.59; H, 2.31; N, 9.83%.

3-(5-bromobenzo[d]isoxazol-3-yl)-2-(4-bromophenyl) thiazolidin-4-one (3h):

IR (KBr): 1715 cm⁻¹ $\nu_{(C=O)}$; ¹H NMR (400 MHz, CDCl₃ δ in ppm) δ 7.821-7.757 (m, 4H, Ar-H), 7.564 (s, 1H, Ar-H), 7.321-7.201 (m, 1H, Ar-H), 6.434 (s, 1H, -S-CH-), 4.202-4.196 (d, $J=2.4$ Hz, 1H, -CH₂-), 4.120-4.114 (d, $J=2.4$ Hz, 1H, -CH₂-); ¹³C NMR (100 MHz, CDCl₃ δ in ppm) δ 171.03, 164.61, 148.20, 138.66, 134.36, 131.92, 130.67, 128.06, 123.06, 121.96, 118.24, 112.28, 73.29, 33.93; ESI-MS m/z 455 [M+H]⁺,]⁺; Anal. Calcd for C₁₆H₁₀N₂O₂BrS: C, 42.32; H, 2.22; N, 6.17; found: C, 42.25; H, 2.16; N, 6.11%.

3-(5-bromobenzo[d]isoxazol-3-yl)-2-(2-butyl-4-chloro-1H-imidazol-5-yl) thiazolidine-4-one (3i):

IR (KBr): 1733 cm⁻¹ $\nu_{(C=O)}$; ¹H NMR (400 MHz, DMSO d₆ δ in ppm) δ 9.9 (s, 1H, -NH-), 7.6 (m, 2H, Ar-H), 7.4 (m, 1H, Ar-H), 6.7 (s, 1H, S-CH-), 4.2 (d, 1H,-CH₂-), 4.0 (d, 1H,-CH₂-), 2.5 (t, 2H, -CH₂-), 1.4 (m, 2H, -CH₂-), 1.2 (m, 2H,-CH₂-), 0.9 (m, 3H, -CH₃); ¹³C NMR (100 MHz, DMSO-d₆ δ in ppm) δ 170.89, 164.25, 148.31, 147.46, 135.29, 127.98, 124.06, 122.68, 118.44, 112.15, 58.79, 34.18, 30.97, 28.54, 22.65, 13.85; ESI-MS m/z 456 [M+H]⁺; Anal. Calcd for

C₁₇H₁₆BrClN₄O₂S: C, 44.80; H, 3.54; N, 12.29; found C, 44.71; H, 3.49; N, 12.22 %.

3-(2-methyl-1H-indol-5-yl)-2-(3-nitrophenyl) thiazolidine-4-one (3j):

IR (KBr): 1720 cm⁻¹ $\nu_{(C=O)}$; ¹H NMR (400 MHz, DMSO d₆ δ in ppm) δ 10.928 (s, 1H, -NH-), 8.203 (s, 1H, Ar-H), 8.126 (m, 1H, Ar-H), 7.907 (m, 1H, Ar-H), 7.573 (m, 1H, Ar-H), 7.255 (s, 1H, Ar-H), 7.141-7.120 (m, 1H, Ar-H), 6.864-6.838 (m, 1H, Ar-H), 6.599 (s, 1H, S-CH-), 6.028 (m, 8H, Ar-H), 4.106-4.102 (d, J = 1.6 Hz, 1H, -CH₂-), 4.067-4.063 (d, J = 1.6 Hz, 1H, -CH₂-), 2.169 (s, 3H, -CH₃-); ¹³C NMR (100 MHz, DMSO-d₆ δ in ppm) δ 169.25, 148.41, 139.66, 134.97, 133.67, 130.29, 128.31, 124.53, 120.12, , 112.92, 108.52, 100.91, 73.49, 35.31, 15.86; ESI-MS m/z 354 [M+H]⁺; Anal. Calcd for C₁₈H₁₅N₃O₃S requires: C, 61.18; H, 4.28; N, 11.89; found: C, 61.11; H, 4.20; N, 11.15%.

2-(4-bromophenyl)-3-(2-methyl-1H-indol-5-yl) thiazolidine-4-one (3k):

IR (KBr): 1722 cm⁻¹ $\nu_{(C=O)}$; ¹H NMR (400 MHz, DMSO d₆ δ in ppm) 10.7 (s, 1H, -NH-), 7.5 (m, 2H, Ar-H), 7.4 (s, 1H, Ar-H), 7.1 (m, 2H, Ar-H), 6.9 (m, 2H, Ar-H), 6.6 (s, 1H, S-CH-), 6.0 (s, 1H, -NCH-), 4.1 (d, 1H, -CH₂-), 4.0 (d, 1H, -CH₂-), 2.3 (s, 3H, -CH₃-); ¹³C NMR (100 MHz, CDCl₃ δ in ppm) δ 171.51, 139.36, 135.86, 134.59, 132.71, 131.22, 130.34, 128.72, 121.99, 112.86, 111.68, 108.92, 102.34, 73.28, 33.84, 13.96; ESI-MS m/z 388 [M+H]⁺; Anal. Calcd for C₁₈H₁₅BrN₂OS C, 55.85; H, 3.90; N, 7.23; found C, 55.69; H, 3.85; N, 7.13 %.

2-(2-butyl-4-chloro-1H-imidazol-5-yl)-3-(2-methyl-1H-indol-5-yl) thiazolidine-4-one (3l):

IR (KBr): 1689 cm⁻¹ $\nu_{(C=O)}$; ¹H NMR (400 MHz, DMSO d₆ δ in ppm) δ 7.7 (s, 1H, Ar-H), 7.2 (s, 1H, Ar-H), 7.0 (s, 1H, Ar-H), 6.1 (s, 1H, S-CH-), 4.2 (d, 1H, -CH₂-), 4.0 (d, 1H, -CH₂-), 2.9 (t, 2H, -CH₂-), 2.4 (s, 2H, -NH-), 2.2 (s, 3H, -CH₃), 1.4 (m, 2H, -CH₂-), 1.2 (m, 2H, -CH₂-), 0.9 (t, 3H, -CH₃); ¹³C NMR (100 MHz, DMSO-d₆ δ in ppm) δ 172.35, 148.05, 134.39, 133.25, 131.57,

128.20, 124.19, 113.57, 108.53, 102.61, 57.91, 34.97, 31.11, 28.52, 22.72, 15.89, 13.28; ESI-MS m/z 389 $[M+H]^+$; Anal. Calcd for $C_{19}H_{21}ClN_4OS$: C, 58.68; H, 5.44; N, 14.41; found: C, 58.55; H, 5.25; N, 14.29%.

3-(1-oxo-1,3-dihydroisobenzofuran-5-yl)-2-(2,4,6-trifluorophenyl)thiazolidin-4-one (3m):

IR (KBr): 1721 cm^{-1} $\nu_{(C=O)}$; ^1H NMR (400 MHz, DMSO d_6 δ in ppm) δ 8.230-8.218 (d, 1H, Ar-H), 7.846-7.825 (d, 1H, Ar-H), 7.237 (s, 1H, Ar-H), 6.518 (s, 1H, S-CH-), 6.326-6.267 (m, 2H, Ar-H), 5.381 (s, 2H, -COCH₂-), 4.411-4.403 (s, $J=3.2$ Hz, 2H, -CH₂-), 4.320-4.312 (d, $J=3.2$ Hz, 1H, -CH₂-); ^{13}C NMR (100 MHz, DMSO- d_6 δ in ppm) δ 171.94, 163.87, 146.01, 144.40, 130.39, 124.72, 121.62, 118.82, 107.45, 100.58, 70.01, 55.42, 35.58; ESI-MS m/z 366 $[M+H]^+$; Anal. Calcd for $C_{17}H_{10}NO_3F_3S$: C, 55.89; H, 2.76; N, 3.83; found: C, 55.78; H, 2.68; N, 3.75%.

2-(4-nitrophenyl)-3-(1-oxo-1,3-dihydroisobenzofuran-5-yl)thiazolidin-4-one (3n):

IR (KBr): 1714 cm^{-1} $\nu_{(C=O)}$; ^1H NMR (400 MHz, DMSO d_6 δ in ppm) δ 8.223-8.167 (m, 1H, Ar-H), 7.743-7.722 (m, 2H, Ar-H), 7.691-7.71 (m, 1H, Ar-H), 7.445-7.403 (m, 3H, Ar-H), 6.576 (s, 1H, S-CH-), 5.188 (s, 2H, -COCH₂-), 3.921-3.917 (d, $J=1.6$ Hz, 1H, -CH₂-), 3.86-3.865 (d, $J=1.6$ Hz, 1H, -CH₂-); ^{13}C NMR (100 MHz, CDCl₃ δ in ppm) δ 171.59, 169.23, 147.28, 146.81, 145.29, 144.88, 131.24, 129.86, 124.20, 122.23, 121.12, 120.01, 73.31, 69.24, 34.18; ESI-MS m/z 357 $[M+H]^+$; Anal. Calcd for $C_{17}H_{12}N_2O_5S$: C, 57.30; H, 3.39; N, 7.86; found: C, 57.19; H, 3.30; N, 7.79%.

2-(4-bromophenyl)-3-(1-oxo-1,3-dihydroisobenzofuran-5-yl)thiazolidin-4-one (3o):

IR (KBr): 1723 cm^{-1} $\nu_{(C=O)}$; ^1H NMR (400 MHz, DMSO d_6 δ in ppm) δ 8.120-8.094 (d, 1H, Ar-H), 7.835-7.819 (d, 1H, Ar-H), 7.508 (s, 1H, Ar-H), 7.412-7.389 (m, 2H, Ar-H), 7.059-7.037 (m,

2H, Ar-H), 6.403 (s, 1H, S-CH-), 5.604 (s, 2H, -COCH₂-), 4.034-4.031 (d, $J=1.2$ Hz, 1H, -CH₂-), 3.892-3.889 (d, $J=1.2$ Hz, 1H, -CH₂-); ¹³C NMR (100 MHz, CDCl₃ δ in ppm) δ 171.61, 169.61, 147.35, 146.41, 138.68, 132.21, 131.83, 130.01, 122.24, 121.73, 120.88, 119.74, 73.16, 33.89; ESI-MS m/z 391 [M+H]⁺; Anal. Calcd for C₁₇H₁₂NO₃BrS: C, 52.32; H, 3.10; N, 3.59; found: C, 52.26; H, 2.91; N, 3.48%.

Antibacterial studies

The antibacterial assay was performed *via* serial dilution method and agar diffusion method at different concentrations new compounds.³¹ All synthesized small molecules were screened for their *in vitro* antibacterial activity against gram-negative bacteria, *S.typhi* (MTCC 733) and *K.pneumoniae* (MTCC 661) by the agar diffusion method at different concentration. The stock cultures of bacteria were revived by inoculating them in broth media and were grown at 37 °C for 18 hours. The agar plates of the above media are prepared and each plates were inoculated with bacterial strains. The wells were made in the plates using cork borer and different concentrations of compounds were added and diameter of the inhibition zone was noted. The MIC values were calculated using serial dilution method.

Cheminformatics analysis

In silico target prediction

Given the constantly increasing amount of bioactivity data available, we attempted to rationalise the mode-of-action of the experimentally active compounds using *in silico* approaches, which is currently the topic of many chemogenomics studies.³² In order to achieve this, we applied the Parzen-Rosenblatt Window classifier (with the smoothing parameter having set to 0.9) to predict potential targets for the compounds which were experimentally tested.²³ This classifier was

trained on a large dataset comprising approximately 190,000 bioactive compounds covering 477 human protein targets. Normalised target likelihood was calculated for each predicted target by comparing the predicted targets in the dataset used in this study to target predictions of a background dataset comprising 3,000 compounds in total from PubChem,³³ GDB13³⁴ and ChEMBL³⁵ with 1,000 compounds randomly selected from each database. All targets with a probability of 0.05 or higher were considered as predicted in both cases. For each predicted target, the normalised likelihood was determined by dividing the relative frequency of the predicted target for the compound by the relative frequency of the prediction of same target in the background dataset:

$$\text{Normalized likelihood}_{\text{target n}} = \frac{f_{n, \text{dataset}}}{f_{n, \text{background}}}$$

Subsequently, a DELTA-BLAST protein domain similarity search³⁶ was performed on the predicted human targets using their respective Swiss-Prot³⁷ identifiers in order to extrapolate from human protein targets to protein targets in *S.typhi*. DELTA-BLAST is a protein sequence alignment algorithm which aims to find homologous proteins across species based on the similarity of their protein domains. The concept of assessing proteins based on the similarity of their domains has been previously explored to predict homologous targets³⁸ and has also been proven suitable for the prediction of novel targets for *M.tuberculosis*.³⁹ In our case, the DELTA-BLAST search was limited to *S.typhi* (taxid:90371) and the UniProtKB/Swiss-Prot database³⁷ was chosen as the search database due to its high quality of manually curated proteins. All searching parameters were set to their respective default values (*i.e.* the expect threshold was set to 0.01, word size was set to 3 and the maximum number of matches in a query range set to 0) and standard scoring parameters were used, namely the BLOSUM62 position specific scoring matrix, the existence of a gap was assigned a score cost of 11, whereas gap extension costs were

set to 1. Compositional adjustments were set to composition-based statistics and the DELTA-BLAST threshold was set to 0.05.

Comparison of bioactivity of compounds similar to compound 3b

Bioactivity data for compounds with a similarity of 70% or higher to compound 3b, based on the Accelrys Direct similarity measure employed by ChEMBL,⁴⁰ were retrieved from ChEMBL.³⁵ Bioactivity data for only compounds with an AC₅₀, EC₅₀, IC₅₀ or potency value of 10 μ M or better and a ChEMBL confidence score of 8 or higher were considered. Subsequently, the set of targets (including duplicates) retrieved were categorised in terms of the PANTHER²⁶ biological processes they are involved in.

Molecular docking:

Molecular modelling was performed in InsightII, Discovery Studio (DS) Version 2.5. The structure and mechanism of hexameric FtsK, a double-stranded DNA was adopted in our docking studies (with the water molecules removed). The generated ligand conformations were energy minimized with the CHARMM force field using steepest descent until convergence. During the final step of docking using the LigandFit program (version 2.5), all the minimised conformations were compared and redundant conformations were discarded. Each docked pose was evaluated for its fitness using multiple scoring functions (LigScore1, LigScore2, -PLP1, -PLP2, Jain, -PMF, Ludi 1, Ludi 2, Ludi 3, -PMF04, DOCK SCORE). Subsequently, the multiple scores obtained from the calculations of LigandFit were prioritized for each docked pose. The docked poses of active compounds among **3(b-o)** with the hydrophobic sites of the FtsK motor domain with the highest consensus score was selected as the favorable conformation and their complex structure was prepared.

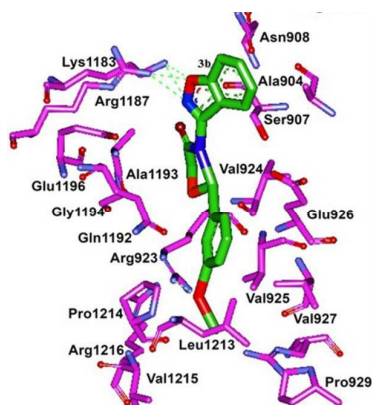
Acknowledgements

This research is supported by the grants from DC-wrangler Pavate Fellowship, University Grants Commission (41-257-2012-SR), Department of Science and Technology, Government of India, to Basappa. Keerthy H K and H Bharathkumar thank the University Grants Commission, New Delhi, India for Basic Science Research fellowship. SP thanks the Netherlands Organisation for Scientific Research (NWO, grant number NWO-017.009.065) and the Prins Bernhard cultuurfonds for funding. Mohan C D thanks the University of Mysore for Department of Science and Technology-Potential of University Research and Scientific Excellence Research Associate Fellowship. AB thanks Unilever for funding.

References

1. R. Sheldon, *Metal-catalyzed oxidations of organic compounds: mechanistic principles and synthetic methodology including biochemical processes*, Elsevier, 2012.
2. N. R. Dighore, P. L. Anandgaonker, S. T. Gaikwad and A. S. Rajbhoj, *Materials Science-Poland*, 2015, **33**, 163-168.
3. D. Parviz, M. Kazemini, A. Rashidi and K. J. Jozani, *Journal of Nanoparticle Research*, 2010, **12**, 1509-1521.
4. Y. Shi, B. Guo, S. A. Corr, Q. Shi, Y.-S. Hu, K. R. Heier, L. Chen, R. Seshadri and G. D. Stucky, *Nano letters*, 2009, **9**, 4215-4220.
5. Y. Zhao, J. Liu, Y. Zhou, Z. Zhang, Y. Xu, H. Naramoto and S. Yamamoto, *Journal of Physics: Condensed Matter*, 2003, **15**, L547.
6. M. K. Dongare, V. V. Bhagwat, C. Ramana and M. K. Gurjar, *Tetrahedron letters*, 2004, **45**, 4759-4762.
7. M. A. Albrecht, C. W. Evans and C. L. Raston, *Green Chemistry*, 2006, **8**, 417-432.
8. L. Lietti, G. Ramis, G. Busca, F. Bregani and P. Forzatti, *Catalysis today*, 2000, **61**, 187-195.
9. S. Anusha, B. Cp, C. D. Mohan, J. Mathai, S. Rangappa, S. Mohan, Chandra, S. Paricharak, L. Mervin, J. E. Fuchs, M. M, A. Bender, Basappa and K. S. Rangappa, *PloS one*, 2015, **10**, e0139798.
10. S. Maisnier-Patin, O. G. Berg, L. Liljas and D. I. Andersson, *Molecular microbiology*, 2002, **46**, 355-366.
11. T. Kline, H. B. Felise, K. C. Barry, S. R. Jackson, H. V. Nguyen and S. I. Miller, *Journal of medicinal chemistry*, 2008, **51**, 7065-7074.
12. T. Kline, K. C. Barry, S. R. Jackson, H. B. Felise, H. V. Nguyen and S. I. Miller, *Bioorganic & medicinal chemistry letters*, 2009, **19**, 1340-1343.
13. C. Kavitha, S. N. Swamy, K. Mantelingu, S. Doreswamy, M. Sridhar, J. S. Prasad and K. S. Rangappa, *Bioorganic & medicinal chemistry*, 2006, **14**, 2290-2299.
14. S. Anusha, B. S. Anandakumar, C. D. Mohan, G. P. Nagabhushana, B. S. Priya, K. S. Rangappa, Basappa and C. G. T, *RSC Advances*, 2014, **4**, 52181-52188.
15. N. Ashwini, M. Garg, C. D. Mohan, J. E. Fuchs, S. Rangappa, S. Anusha, T. R. Swaroop, K. S. Rakesh, D. Kanojia, V. Madan, A. Bender, H. P. Koeffler, Basappa and K. S. Rangappa, *Bioorg Med Chem*, 2015, **23**, 6157-6165.

16. M. Neelgundmath, K. R. Dinesh, C. D. Mohan, F. Li, X. Dai, K. S. Siveen, S. Paricharak, D. J. Mason, J. E. Fuchs, G. Sethi, A. Bender, K. S. Rangappa, O. Kotresh and Basappa, *Bioorg Med Chem Lett*, 2015, **25**, 893-897.
17. H. Bharathkumar, C. D. Mohan, H. Ananda, J. E. Fuchs, F. Li, S. Rangappa, M. Surender, K. C. Bulusu, K. S. Girish, G. Sethi, A. Bender, Basappa and K. S. Rangappa, *Bioorg Med Chem Lett*, 2015, **25**, 1804-1807.
18. K. S. Rakesh, S. Jagadish, A. C. Vinayaka, M. Hemshekhar, M. Paul, R. M. Thushara, M. S. Sundaram, T. R. Swaroop, C. D. Mohan, Basappa, M. P. Sadashiva, K. Kemparaju, K. S. Girish and K. S. Rangappa, *PLoS one*, 2014, **9**, e107182.
19. H. Bharathkumar, C. D. Mohan, S. Rangappa, T. Kang, H. Keerthy, J. E. Fuchs, N. H. Kwon, A. Bender, S. Kim and K. S. Rangappa, *Organic & biomolecular chemistry*, 2015, **13**, 9381-9387.
20. C. D. Mohan, H. Bharathkumar, K. C. Bulusu, V. Pandey, S. Rangappa, J. E. Fuchs, M. K. Shanmugam, X. Dai, F. Li, A. Deivasigamani, K. M. Hui, A. P. Kumar, P. E. Lobie, A. Bender, Basappa, G. Sethi and K. S. Rangappa, *The Journal of biological chemistry*, 2014, **289**, 34296-34307.
21. G. Nagabhushana, D. Samrat and G. Chandrappa, *RSC Advances*, 2014, **4**, 56784-56790.
22. B. Matharu, M. Manrao and V. Kaul, *Indian Journal of Heterocyclic Chemistry*, 2005, **15**, 95-96.
23. A. Koutsoukas, R. Lowe, Y. Kalantarmotamedi, H. Y. Mussa, W. Klaffke, J. B. Mitchell, R. C. Glen and A. Bender, *Journal of chemical information and modeling*, 2013, **53**, 1957-1966.
24. L. N. Csonka, *Journal of bacteriology*, 1982, **151**, 1433-1443.
25. M. McClelland, K. E. Sanderson, J. Spieth, S. W. Clifton, P. Latreille, L. Courtney, S. Porwollik, J. Ali, M. Dante and F. Du, *Nature*, 2001, **413**, 852-856.
26. H. Mi, A. Muruganujan and P. D. Thomas, *Nucleic acids research*, 2013, **41**, D377-D386.
27. C. Lesterlin, C. Pages, N. Dubarry, S. Dasgupta and F. Cornet, 2008.
28. N. Dubarry, C. Possoz and F. X. Barre, *Molecular microbiology*, 2010, **78**, 1088-1100.
29. N. P. Higgins, S. Deng, Z. Pang, R. Stein, K. Champion and D. Manna, *Domain behavior and supercoil dynamics in bacterial chromosomes*, Washington, DC: American Society for Microbiology Press, 2005.
30. S. C. Ip, M. Bregu, F. X. Barre and D. J. Sherratt, *The EMBO journal*, 2003, **22**, 6399-6407.
31. J. Löwe, A. Ellonen, M. D. Allen, C. Atkinson, D. J. Sherratt and I. Grainge, *Molecular cell*, 2008, **31**, 498-509.
32. E. van der Horst, J. E. Peironcelly, G. JP van Westen, O. O van den Hoven, W. RJD Galloway, D. R Spring, J. K Wegner, H. WT van Vlijmen, A. P IJzerman and J. P Overington, *Current topics in medicinal chemistry*, 2011, **11**, 1964-1977.
33. Y. Wang, J. Xiao, T. O. Suzek, J. Zhang, J. Wang, Z. Zhou, L. Han, K. Karapetyan, S. Dracheva and B. A. Shoemaker, *Nucleic acids research*, 2012, **40**, D400-D412.
34. L. C. Blum and J.-L. Reymond, *Journal of the American Chemical Society*, 2009, **131**, 8732-8733.
35. A. Gaulton, L. J. Bellis, A. P. Bento, J. Chambers, M. Davies, A. Hersey, Y. Light, S. McGlinchey, D. Michalovich and B. Al-Lazikani, *Nucleic acids research*, 2012, **40**, D1100-D1107.
36. G. M. Boratyn, A. Schaffer, R. Agarwala, S. F. Altschul, D. J. Lipman and T. L. Madden, *Biol Direct*, 2012, **7**, 12.
37. A. Bairoch, B. Boeckmann, S. Ferro and E. Gasteiger, *Briefings in bioinformatics*, 2004, **5**, 39-55.
38. A. Bender, D. Mikhailov, M. Glick, J. Scheiber, J. W. Davies, S. Cleaver, S. Marshall, J. A. Tallarico, E. Harrington and I. Cornella-Taracido, *Journal of proteome research*, 2009, **8**, 2575-2585.
39. P. Prathipati, N. L. Ma, U. H. Manjunatha and A. Bender, *Journal of proteome research*, 2009, **8**, 2788-2798.
40. A. D. Accelrys Software Inc., Release 8.0, San Diego: Accelrys Software Inc., 2013.



Thiazolidin-4-ones inhibits bacterial growth by targeting FtsK motor domain of DNA translocase of *Salmonella typhi*